HHS Public Access

Author manuscript

Toxicol In Vitro. Author manuscript; available in PMC 2018 June 01.

Published in final edited form as:

Toxicol In Vitro. 2017 June ; 41: 223–231. doi:10.1016/j.tiv.2017.03.002.

Evaluation of multiwalled carbon nanotube cytotoxicity in cultures of human brain microvascular endothelial cells grown on plastic or basement membrane

Brittany N. Eldridge[1], **Fei Xing**[1], **Cale D. Fahrenholtz**[1], and **Ravi N. Singh**[1,2,*]

[1]Department of Cancer Biology, Wake Forest School of Medicine, Winston Salem, NC, 27157, USA;

[2]Comprehensive Cancer Center of Wake Forest School of Medicine, Winston Salem, NC 27157, USA

Abstract

There is a growing interest in the use of multiwalled carbon nanotubes (MWCNTs) to treat diseases of the brain. Little is known about the effects of MWCNTs on human brain microvascular endothelial cells (HBMECs), which make up the blood vessels in the brain. In our studies, we evaluate the cytotoxicity of MWCNTs and acid oxidized MWNCTs, with or without a phospholipid-polyethylene glycol coating. We determined the cytotoxic effects of MWCNTs on both tissue-mimicking cultures of HBMECs grown on basement membrane and on monolayer cultures of HBMECs grown on plastic. We also evaluated the effects of MWCNT exposure on the capacity of HBMECs to form rings after plating on basement membrane, a commonly used assay to evaluate angiogenesis. We show that tissue-mimicking cultures of HBMECs are less sensitive to all types of MWCNTs than monolayer cultures of HBMECs. Furthermore, we found that MWCNTs have little impact on the capacity of HBMECs to form rings. Our results indicate that relative cytotoxicity of MWCNTs is significantly affected by the type of cell culture model used for testing, and supports further research into the use of tissue-mimicking endothelial cell culture models to help bridge the gap between in vitro and in vivo toxicology.

Keywords

Toxicity; angiogenesis; nanoparticle; extracellular matrix; blood brain barrier

*To whom correspondence should be addressed: Ravi Singh, Ph.D., Assistant Professor, Department of Cancer Biology, Wake Forest University Health Sciences, Hanes Bldg., Rm. 4045, Medical Center Blvd., Winston-Salem, NC 27157; Phone: 336-713-4434; FAX: 336-716-0255; rasingh@wakehealth.edu.

Disclosure Statement:
There are no competing financial interests to declare.

Conflict of Interest: There are no competing financial interests to declare.

Introduction

Carbon nanotubes (CNTs) are a heterogeneous class of nanomaterials that consist of sheets of sp^2 hybridized carbon formed into single- or multi- walled tubes (termed SWCNTs or MWCNTs, respectively), which can be further modified by covalent or non-covalent functionalization of their surfaces(Chen et al., 2011). Their unique combination of electrical, thermal and spectroscopic properties offer opportunities for advances in biomedical science including new ways to detect, monitor and treat diseases(Alshehri et al., 2016; Madani et al., 2011; Singh and Torti, 2013). CNTs readily pass through cell membranes due to their unique needle-like structure(Al-Jamal et al., 2011b; Lacerda et al., 2013; Lacerda et al., 2012), and can be used to deliver drugs or nucleic acids to cells(Pantarotto et al., 2004; Singh et al., 2005).

There is a growing interest in the development of CNTs to treat neurological damage and brain disease(Ouyang et al., 2016; Zhao et al., 2011). Potential applications of CNTs in the brain include their use as scaffolds to support neuronal growth and enhance the performance of synaptic interfaces(Cellot et al., 2009), as vectors for intracerebral delivery of nucleic acids to reduce damage and improve recovery following stroke(Al-Jamal et al., 2011a; Lee et al., 2011), and as platforms to display antigens to enhance immune responses against gliomas(Zhao et al., 2011). CNTs generate tremendous heat upon exposure to near infrared radiation, making them useful for photothermal cancer therapy(Burke et al., 2012; Singh and Torti, 2013). We and others demonstrated the potential to use CNTs for photothermal treatment of glioblastoma, a deadly brain tumor(Eldridge et al., 2016; Santos et al., 2014; Wang et al., 2011).

For all of these applications, CNTs must be introduced to the brain, either by crossing the blood brain barrier (BBB) or by direct infusion, and toxicity is a concern. Studies investigating nanoparticles in the central nervous system (CNS) have found that diverse cytotoxic effects occur in the CNS after exposure to nanoparticles of various materials (Leite et al., 2015). Even gold nanoparticles, widely considered to exhibit little toxicity and high biocompatibility, can induce neurotoxic effects (Jung et al., 2014), which emphasizes the need for rigorous studies evaluating the potential neurotoxicity of nanomaterials. The cytotoxicity due to CNT exposure has been evaluated in various brain cell types including microglia,(Bardi et al., 2013; Bussy et al., 2015) astrocytes(Meng et al., 2013; Min et al., 2015; Zhang et al., 2011) and neurons(Bussy et al., 2015; Lee et al., 2011). The outcomes of these studies vary widely with some research indicating that CNTs are generally safe while others find CNTs to be cytotoxic and induce inflammation. The cytotoxicity of CNTs is dependent upon the dose and specific type of CNT being tested(Bardi et al., 2013), the type of cell(Bussy et al., 2015), and the biological context (i.e. the microenvironment) in which the test is performed(Burke et al., 2011; Singh and Torti, 2013). Furthermore, an emerging challenge to clinical translation of biomedical nanotechnology is the growing realization that cytotoxicity assays commonly used to evaluate small molecules may not accurately predict the *in vivo* toxicity of nanomaterials. For example, CNTs are known to interfere with commonly used viability assays such as MTT, leading to inaccurate estimates of toxicity (Herzog et al., 2007; Worle-Knirsch et al., 2006). More significantly, cytotoxicity assays using cells grown on standard laboratory plastics fail to recapitulate the complex

morphology, diffusional barriers and altered cell signaling that are present in tissue(Krug and Wick, 2011; O'Brien et al., 2002; Pampaloni et al., 2007; Worle-Knirsch et al., 2006; Yamada and Cukierman, 2007), all of which may affect responses to nanomaterials. New cell culture techniques are being developed which enable cells to organize into tissue-like structures that better recapitulate an *in vivo* setting(O'Brien et al., 2002; Pampaloni et al., 2007; Yamada and Cukierman, 2007). Several studies have shown striking differences in nanoparticle cytotoxicity between treatment of cells grown as a monolayer on plastic versus cells cultured under conditions where they are able to form tissue-like structures(Behan et al., 2011; Chia et al., 2015; Movia et al., 2011).

Brain microvasculature plays a crucial role in supporting brain homeostasis, but little is known about the effects of CNTs on brain microvascular endothelium. The integrity of the endothelium of the microvasculature is an essential aspect of the BBB. CNTs can cross the BBB(Kafa et al., 2016; Kafa et al., 2015), but the *in vitro* studies used porcine vascular endothelial cells, which may differ from human cells in their response to CNTs. Isolated human brain microvascular endothelial cells (HBMECs) grown on an extracellular matrix derived substrate (e.g. Matrigel®) will organize into a lattice of ring-like structures similar to small blood vessels(Arnaoutova and Kleinman, 2010). In contrast, HBMECs form a homogeneous monolayer without any tissue-level organization when grown on laboratory plastic. It is unknown if CNT cytotoxicity differs between HBMECs grown as monolayers or under microvessel-forming conditions on basement membrane.

One challenge to these tests is the lack of a validated assay to quantitatively evaluate the cytotoxicity of CNTs using cells grown on basement membrane or extracellular matrix. Therefore, in this report, we describe the development of a modified CellTiter-Glo®-based assay to evaluate the cytotoxicity of CNTs on HBMECs grown in monolayer or on Matrigel®, and validate our results by western blot for cleaved PARP (Poly ADP ribose polymerase), a marker of apoptosis(Boulares et al., 1999). For these studies, we focused on the cytotoxicity of MWCNTs. Because MWCNTs are commonly acid treated or coated in surfactants like phospholipid-polyethylene glycol to improve their dispersion in water and to enhance their diffusion through extracellular matrix(Eldridge et al., 2016), we determined the influence of these modifications on MWCNT cytotoxicity. Furthermore, we examined the effect of MWCNTs on the capacity for HBMECs to form microvascular tubes. These studies contribute to the field of nanotoxicology by determining the impact of MWCNTs on HBMECs and through the development of effective methods to evaluate MWCNT cytotoxicity *in vitro* using cells grown on basement membrane.

Materials and Methods

Cell Culture

Human Brain Microvasculature Endothelial Cells (HBMECs) from Angio-Proteomie were maintained in Endothelial Cell Basal Medium-2 (EBM-2) (Lonza) supplemented with EGM™-2 SingleQuots® (Lonza) at 37 °C under 5% CO_2 in a humidified incubator. Alternatively, HBMECs were seeded on solidified Corning® Matrigel® Growth Factor Reduced (GFR) Basement Membrane Matrix (Corning). MDA-MB-231 breast cancer cells were purchased from ATCC (American Type Culture Collection). MDA-MB-231 cells were

grown in DMEM supplemented with 10% FBS (vol:vol), 2 mM L-glutamine, penicillin (250 U/mL), and streptomycin (250 μg/mL) (all from Invitrogen).

Preparation of MWCNT dispersions

Short multiwalled carbon nanotubes (MWCNTs) 8–15 nm in diameter were purchased from Nanostructured & Amorphous Materials, Inc. Acid treatment and purification of the MWCNTs was performed as we previously described(Fahrenholtz et al., 2015). DSPE-PEG_{5000} (Nanocs, Inc.) was dissolved at a concentration of 2% weight to volume in deionized water. Dispersions of MWCNTs were prepared by adding 10 mg of unmodified or acid oxidized MWCNTs to 10 mL of Milli-Q (type I) water or 2% DSPE-PEG solution in a 20 mL glass vial, followed by 30 minutes of bath sonication at 40 Hz (Branson 2510) at 4 °C, with vials placed to produced maximal resonance waves of the solution. Prior to use in cell culture, the MWCNT suspensions were rendered isotonic by the addition of one part in 10 of 10× phosphate-buffered saline (PBS) (Invitrogen).

Physiochemical Characterization of MWCNTs by Dynamic Light Scattering

Hydrodynamic diameter and ζ-potential were measured using the Zetasizer Nano ZS90 (Malvern Instruments) at 25 °C, with automatic settings, adjusting for the refractive index and viscosity of the dispersant. The particles were diluted to 5 μg/mL and 1 mL was added to a disposable, clear plastic cuvette (Sarstedt) or a disposable folded capillary zeta cell (Malvern Instruments). Each measurement was taken in triplicate.

Optical Absorbance Spectroscopy

MWCNTS were diluted to the indicated concentrations in 500 μL of a 1:1 PBS:CellTiter-Glo® solution and transferred to a glass cuvettes. Absorbance measurements were taken at 700 nm using a Spectronic 200 (ThermoScientific) spectrophotometer.

CellTiter-Glo® Assay

MDA-MB-231 (5,000 cells/well) or HBMECs (10,000 cells/well) were seeded into 96 well plates on plastic or Matrigel® and allowed to recover for 24 h. Cells were treated with MWCNTs for 24 h. After MWCNT treatment, cell culture media was removed and replaced with a 1:1 mixture of 1xPBS and CellTiter-Glo® reagent. Samples were incubated at room temperature for 10 minutes in the dark. The resulting solution was mixed, centrifuged for 5 min at 13,000 × G to remove MWCNTs. The supernatant was transferred to Microtiter™ Microlite™ White Strip Plates (Thermo Scientific), and total luminescence was measured using a Tecan GENios microplate reader.

Cleaved PARP Western Blot

Lysates were collected using triton lysis buffer (20 mM Tris-HCl, 5 mM EDTA, 1% Triton X 100, pH 8.3) supplemented with 1% Halt™ Protease & Phosphatase Inhibitor Cocktail (Thermo Scientific). For HBMECs grown on Matrigel®, cells were isolated by aspirating normal growth media and adding equivalent culture volumes of Dispase (Corning), incubating at 37 °C for 30 min, then washing 2x with ice cold 1xPBS prior to lysis. Protein concentration was determined for each sample using a Bicinchoninic acid (BCA) protein

assay kit (Thermo-Fisher/Pierce). Next, 5–10 μg of protein lysate were subjected to sodium dodecyl sulfate polyacrylamide gel electrophoresis (SDS-PAGE) on a 12% Ready Gel® Tris-HCl gels (Bio-Rad) and transferred to nitrocellulose (Bio-Rad). Membranes were blocked with 5% non-fat milk solution in tris-buffered saline (TBS) with 1% Tween 20 (Sigma-Aldrich) for 30 minutes. Blots were probed with antibodies diluted in 5% BSA or 5% milk. Antibodies (Cell Signaling Technology) were diluted to the following concentrations: c-PARP (1:1000) and GAPDH (1:10,000) in 5% milk or BSA according to manufacturer's protocol. Membranes were developed using SuperSignal® West Pico Chemiluminescent Substrate (Thermo Scientific).

^{3}H-MWCNT Uptake Assay

Radiolabeled MWCNTs were prepared using methods similar to those we previously described(Fahrenholtz et al., 2015). Acid oxidized MWCNTs (20 mg) were dispersed in 4 ml of deionized water by bath sonication as described above. To this dispersion, 1 ml of a 10 mg/ml solution of 1-ethyl-3-(3-dimethylaminopropyl)carbodiimide hydrochloride (EDC; Thermo Scientific) was added. The solution was stirred at room temperature for 15 min then 100 μl of tritiated (^{3}H) glucosamine (^{3}H-GlcN; 1 mCi/ml in water; Perkin Elmer) and 2 mg of Sulfo-NHS (N-hydroxysulfosuccinimide; Thermo Scientific) were added. A 1/10th volume of 10X PBS (Invitrogen) was added to increase the pH to 7.4 and the reaction was allowed to proceed overnight at 4 °C. The reaction mixture was washed three times then concentrated to a 1 ml volume using 100K MWCO centrifuge columns (EMD Millipore). Any remaining unreacted chemicals were removed by purification using a PD-10 column and deionized water as the running buffer. The flow through was collected in 15 fractions (500 μl each) and radioactivity in 50 μl of each fraction was quantified in 15 ml of Ecolume scintillation cocktail (MPBio) using a Beckman LS5000 scintillation counter. Fractions 2 and 3 were found to contain approximately 95% of the total radioactivity and were dark black, indicative of MWCNTs. Any remaining unconjugated ^{3}H-GlcN was separated from the ^{3}H-MWCNTs using 100K MWCO centrifuge columns (EMD Millipore), and the radiochemical purity of the ^{3}H-MWCNTs was determined to be greater than 98%. The ^{3}H-MWCNTs were used without further modification or coated in 2% DSPE-PEG as described above. HBMECs were plated in 24-well tissue culture plates (1.3×10^{5} cells/well). The following day, cells were treated with uncoated ^{3}H-MWCNT, DSPE-PEG coated ^{3}H-MWCNT, or vehicle at the indicated doses for the specified times. Cells were washed twice in ice cold 1xPBS, harvested in 200 μl of lysis buffer (20 mM TRIS, 0.1M NaCl, 2% Triton-X, 10 mM EDTA), and ^{3}H activity was assessed as described above. Prior to lysis, photomicrographs of ^{3}H-MWCNT-treated cell cultures were obtained using a Moticam 3 digital camera mounted on a VWR VistaVision microscope at 10x magnification.

HBMEC-Vessel Formation Assay

HBMECs were grown as a monolayer (50,000 cells/well) in a 24 well plate, and then were treated with 25 μg/mL MWCNTs for 16 hr. The cells were then washed, trypsinized, counted and plated in vessel forming conditions. To form HBMEC vessels, Matrigel (35 μL per well) was added to wells of a 96 well plate at a final concentration of 9.8 mg/mL and allowed to solidify at 37 °C for ~20 min. Once matrigel solidified, HBMECs were plated at a density of 4,000–10,000 cells per well and allowed to form vessel-like structures.

HBMECs were treated with 25 μg/mL of each MWCNT preparation. Changes in morphology of vessel-like structures were monitored over time and photographed using Invitrogen EVOS FL Auto Imaging System (Thermo Fisher) at the indicated time points.

Results

Characterization of MWCNTs

Four different aqueous dispersions of MWCNTs were generated: (1) Uncut/ Uncoated MWCNTS dispersed by sonication in water; (2) Uncut/Coated, which are MWCNTs dispersed in 2% weight to volume aqueous solution of 1,2-distearoyl-sn-glycero-3-phosphoethanolamine-N-amino(polyethylene glycol)$_{5000}$ (DSPE-PEG); (3) Cut/Uncoated, which are MWCNTs that were oxidized and shortened by acid treatments; and (4) Cut/ Coated: MWCNTs that were oxidized and shortened by acid treatments then dispersed in a 2% DSPE-PEG solution. The four MWCNT preparations were analyzed using dynamic light scattering (DLS) to determine the hydrodynamic diameter and ζ-potential. In water, all four suspensions exhibited monomodal size distributions (Table 1 and Supplemental Fig. S1).

Acid oxidized (cut) MWCNTs were smaller compared to uncut MWCNTs, and DSPE-PEG coated MWCNTs (cut and uncut) were larger than equivalent uncoated MWCNTs due to the PEG polymer (Table 1). When suspended in PBS, the hydrodynamic diameter of uncut/ uncoated MWCNTs increased from 185 ± 2 nm in water to 2086 ± 333 nm in PBS (Supplemental Fig S1A). Similarly, the hydrodynamic diameter of cut/uncoated MWCNTs increased from 137 ± 0.1 nm in water to 709 ± 126 nm in PBS (Supplemental Fig S1B). The increase in hydrodynamic diameter is indicative of nanoparticle aggregation and decreased stability in a solution. In contrast, the hydrodynamic diameter of DSPE-PEG coated MWCNTs (both cut and uncut) did not increase after suspension in PBS as compared to water (Table 1, Supplementary Fig S1C, D). ζ-potential measurements show that DSPE-PEG coated MWCNTs (cut and uncut) are less negatively charged (more neutral) compared to equivalent uncoated MWCNTs, indicating that there is the expected charge shielding due to the DSPE-PEG coating. Taken together, the characterization data show that DSPE-PEG coated MWCNTs, irrespective of size, are more colloidally stable in physiologic solutions compared to uncoated MWCNTs and that acid oxidation ‘cuts’ the MWCNTs to shorter lengths.

Optimization and validation of modified CellTiter-Glo® assay to quantify MWCNT cytotoxicity

CellTiter-Glo® is a commercial cell viability assay that quantifies cellular ATP via luminescence produced by a coupled luciferase reaction and is readily adapted for use with cells grown on plastic or on basement membrane. However, MWCNTs absorb light, and may interfere with luminescence measurements. We evaluated the extent to which MWCNTs interfere with the assay. Because HBMECs survive only a finite number of passages, MDA-MB-231 breast cancer cells were used for optimization studies. We first determined if MWCNTs quenched light emission. Untreated MDA-MB-231 cells were lysed in a 1:1 mixture of PBS:CellTiter-Glo® reagent and aliquoted to microcentrifuge tubes. Triplicate tubes of the lysate were spiked with MWCNTs (0, 1, 5, 10, or 25 μg/mL in a 250

μL volume). After addition of MWCNTs, 100 μL of each sample was transferred to a 96 well, white sided plate. The remainder of each sample was centrifuged for 5 min at 13,000 × G to pellet MWCNTs, and then 100 μL of the supernatant was transferred to empty wells. A high concentration of MWCNTs interferes with luminescence measurements prior to centrifugati on to remove MWCNTs, leading to significant decreases in the detected luminescence signal as MWCNT concentration increase (Supplementary Fig S2). Centrifugation of each sample prior to reading luminescence reduced the effect of the MWCNTs, but despite this improvement, higher concentrations of MWCNTs still decreased the signal detected in spiked samples.

The conditions tested above represented a 'worst case scenario' in which all MWCNTs initially added to a well were present during the analysis by CellTiter-Glo®. In practice, only a fraction of the MWCNTs initially added to a well will be associated with the cells and most will be removed by washing prior to cell lysis. We therefore performed an experiment to determine if the amount of MWCNTs present during a conventional CellTiter-Glo® assay was likely to interfere with the assay. MDA-MB-231 breast cancer cells were exposed to increasing concentrations of MWCNTs for 24 h. Subsequently, the MWCNT containing culture media was removed and replaced with a 1:1 mixture of 1xPBS and CellTiter-Glo® reagent. The resulting solution was mixed and centrifuged for 5 min at 13,000 × G to remove MWCNTs. The supernatant was transferred to 1 mL glass cuvettes and optical absorbance was measured at a wavelength of 700 nm. To determine the amount of MWCNTs present in each sample, a standard curve was generated by spiking known amounts (0 – 50 μg/mL) of MWCNTs into a 1:1 mixture of 1xPBS and CellTiter-Glo® reagent. Optical absorbance readings for cells treated with 0 – 25 μg/mL MWCNTs indicate very few MWCNTs were present in samples at the time of measurement (Supplementary Fig S3). The luminescence of each sample was measured by the CellTiter-Glo® assay (Supplementary Fig S4). Cells treated with all four MWCNT preparations show dose dependent decreases in luminescence. The decrease caused by treatment with both types of DSPE-PEG coated MWCNTs was significantly greater than the effect of uncoated MWCNTs. Because the MWCNTs remaining in each sample were not detectable by optical absorbance measurements, we concluded that the observed decrease in luminescence was due to loss of cell viability after MWCNT treatment and not due to interference of MWCNTs with the luminescence viability assay.

Evaluation of cytotoxicity and apoptotic response in HBMECs grown on plastic or Matrigel® following exposure to MWCNTs

Having validated the capacity to use the CellTiter-Glo® assay (with an additional centrifugation step) to quantify the cytotoxicity of MWCNTs, we next examined if the cytotoxicity caused by MWCNTs differed between treatment of monolayer cultures of HBMECs grown on plastic or tissue-mimicking cultures of HBMECs grown on basement membrane (Matrigel). After 24 h of MWCNT treatment, HBMECs grown on plastic exhibited a dose dependent decrease in viability following exposure to all types of MWCNTs, but both types of DSPE-PEG coated MWCNTs were significantly more cytotoxic than uncoated MWCNTs, with Uncut Coated being the most toxic (Fig 1A). Strikingly, HBMECs grown on Matrigel were less sensitive to MWCNT exposure and

similar cytotoxicity was observed among treatments with all four MWCNT preparations (Fig 1B).

Because reduced ATP levels indicated by the CellTiter-Glo® assay may be indicative of decreased cell metabolism and not only decreased cellular viability, we further investigated the ability of MWCNTs to induce cell death of HBMECs. To support the findings that MWCNTs were causing cell death and not just decreased cell metabolism, whole cell lysates from the treatment groups described above were collected and immunoblotted for cleaved PARP, which is indicative of apoptosis. Notably, HBMECs grown on plastic exhibited an increase in cleaved PARP in response to treatment with DSPE-PEG coated MWCNTs while little change in cleaved PARP was observed for cells treated with uncoated MWCNTs (both cut and uncut) (Fig 1C and Fig S5A, B). For HBMECs grown on plastic, DSPE-PEG coated-MWCNTs induce apoptosis to a greater extent than uncoated MWCNTs, which is consistent with the cytotoxicity data for cells grown on plastic. Also in agreement with the cytotoxicity data, HBMECs grown on Matrigel showed no increase in cleaved PARP following treatment with all four types of MWCNTs (Fig 1D and Fig S5C, D). Taken together, these data showed that growth conditions substantially affect the sensitivity of HBMECs to MWCNTs.

Evaluation of cellular uptake of uncoated and coated MWCNTs

Acid oxidized MWCNTs can be easily radiolabeled by conjugation of ^{3}H-glucosamine to carboxylic acids on the MWCNTs surface as described in the Methods section. We previously showed that conjugation of glucosamine to the MWCNT surface does not affect the cell binding affinity or uptake of the MWCNTs(Fahrenholtz et al., 2015). To evaluate whether the observed increased toxicity of coated MWCNTs compared to uncoated MWCNTs was due to differences in cellular uptake, HBMECs were plated on plastic in monolayer and were exposed to cut uncoated or cut coated ^{3}H-MWCNT. At various time points (5 min to 24 h), cells were washed thoroughly to remove ^{3}H-MWCNT that were not bound or taken up by cells. Cells were then lysed and ^{3}H activity in the lysate was assessed by scintillation counting. Both uncoated and DSPE-PEG coated ^{3}H-MWCNTs exhibited a time dependent increase in binding/uptake; however, the uncoated ^{3}H-MWCNTs showed a much higher cell association compared to coated ^{3}H-MWCNTs (Fig 2A). This is drastic increase in cell binding/uptake of uncoated ^{3}H-MWCNTs relative to coated ^{3}H-MWCNTs is most likely due to the increased aggregation and sedimentation of the uncoated MWCNTs (Fig 2B) as a result of their poor colloidal stability in physiologic solutions compared to the DSPE-PEG coated MWCNTs, which remained well dispersed as shown in Supplementary Figure S1. These results suggest that higher cell binding/uptake of MWCNTs does not necessarily correlate with increased toxicity in HBMEC monolayers.

Evaluation of MWCNT effects on microvessel formation and degradation

Carbon nanomaterials can inhibit(Wierzbicki et al., 2013) or enhance(Meng et al., 2015) angiogenesis depending on the properties of the nanomaterial under investigation. Therefore, we investigated the potential effects of MWCNTs on the capacity of HBMECs to initiate vessel formation. We first treated HBMECs grown as a monolayer with 25 μg/mL of each of our four MWCNT preparations. After 16 h, the MWCNT-treated HBMECs were trypsinized, counted and 10,000 cells/well were plated on Matrigel to induce formation of

vessel-like structures (rings). Ring formation was quantified 6 h later (Fig 3A and Fig S6). Despite inducing significant cytotoxicity in HBMEC monolayers at this dose, Cut Coated MWCNTs did not affect ring formation. Uncut uncoated MWCNTs increased the number of rings observed (Fig 3B), which may be a result of potential pro-angiogenic effects that are reported to be induced by some types of CNTs(Azad *et al.*, 2013). Alternatively, aggregates formed by the uncoated MWCNTs are apparent in the photomicrographs. Incorporation of these aggregates into the extracellular matrix may act as a good substrate for endothelial growth. This would be consistent with findings showing improved neuronal growth on MWCNT-loaded scaffolds (Lee and Parpura, 2009; Mattson et al., 2000). However, treatment of monolayer grown HBMECs with Uncut Coated MWCNTs, which were the most cytotoxic to monolayer cells, decreased the number of rings that formed. These data support the idea that HBMEC-basement membrane interactions can mitigate MWCNT cytotoxicity even in cells that previously were exposed to a toxic dose of MWCNTs. However, if the initial damage was sufficiently high (i.e. treatment with Uncut Coated MWCNTs), cells may not recover.

To evaluate the effects of MWCNTs on pre-established vessel-like structures, 4,000 HBMECs per well were plated in tube forming conditions on Matrigel, treated with 25 μg/mL MWCNTs, and ring number was monitored over time. Images taken after 6 h or 16 h of MWCNT treatment showed no effect on the morphology or number of HBMEC vessel rings compared to control (Fig 4A and B; Fig S7). There was a decrease in the number of rings after 16 h (compared to 6 h) due to the expected degradation of the vessels over time(Brown *et al.*, 2016). However, MWCNTs did not significantly affect number of rings compared to control at 16 h (Fig 4C). Thus, MWCNTs did not alter the morphology or increase the rate of degradation of established HBMEC vessel-like structures.

Discussion

In order to advance the development of MWCNTs for treatment of brain disease, it is essential to understand potential cytotoxic effects due to MWCNT exposure. MWCNT functionalization and the resulting effects on colloidal stability of nanoparticles are of particular importance in toxicology studies because these factors influence how particles interact with the cells under investigation(Bardi et al., 2013; Cho et al., 2014; Nafee et al., 2009; Truong et al., 2011; Wang et al., 2016). However, the cell microenvironment may also be an important variable. Here, we find that the cytotoxicity of MWCNTs toward HBMECs is significantly greater when cells are grown on plastic as compared to cells grown on Matrigel, regardless of MWCNT functionalization.

Evaluation of MWCNT cytotoxicity can be challenging because MWCNTs and other nanoparticles often times interfere with cytotoxicity assays(Krug and Wick, 2011; Monteiro-Riviere et al., 2009; Worle-Knirsch et al., 2006). For example, studies have shown that CNTs are incompatible with the MTT assay, a common technique to evaluate cell viability (Worle-Knirsch et al., 2006). CellTiter-Glo® is a viability assay that relies on the ATP-dependent luciferase reaction to produce luminescent oxyluciferin, resulting in a luminescent readout that is correlated with the amount of cellular ATP present. This assay offers an advantage over other common viability assays because it is readily adapted to evaluate viability of cells

grown in three dimensional cultures. Although it is known that CNTs can quench luminesence(Palencia et al., 2015), prior to our studies, it was unknown what impact MWCNTs had on the accuracy of CellTiter-Glo® luminescence measurements. We show that an additional centrifugation step after cell lysis is sufficient to remove MWCNT interference from the assay.

Cell growth conditions can dramatically influence the outcomes of toxicity assays, and we show that MWCNT treatment of HBMECs grown in three-dimensional cell culture conditions does not affect HBMEC viability. These results emphasize the importance of cell environment as an essential variable to consider in future studies evaluating nanoparticle toxicity, including MWCNT toxicity. Several groups have identified novel *in vitro* 3D cell culture techniques to recapitulate tissue-like structures that can provide a more accurate evaluation of nanomaterial toxicity (Dubiak-Szepietowska et al., 2016; Lee et al., 2009; Muoth et al., 2016; Stocke et al., 2017; Wills et al., 2016). More specifically in regards to MWCNT toxicity, and in agreement with our findings, investigators using Schwann cells grown as monolayers or using cells embedded in CNT-loaded scaffolds(Behan et al., 2011) concluded that SWCNTs decreased proliferation and altered Schwann cell morphology in a monolayer, whereas exposure to SWCNTs in a 3D scaffold did not affect cell proliferation, viability, or morphology. Others evaluated SWCNT cytotoxicity using THP1 monocytes and showed that SWCNTs were cytotoxic to THP1 cells grown in 2D cell culture conditions but were not cytotoxic to cells grown in the 3D tissue-mimetic model(Movia et al., 2011). PEG functionalized SWCNTs also did not induce significant morphological alterations in rat hippocampus(Dal Bosco et al., 2015). Similarly, we found that DSPE-PEG coated, acid oxidized MWCNTs were cytotoxic to glioblastoma cells grown in two-dimensional monolayer, but had no observable effect on growth of glioblastoma cells grown as three-dimensional spheroids(Eldridge et al., 2016). However, astrocytes exposed to PEG functionalized SWCNTs may mature and increase glial cell activity(Gottipati et al., 2015). Thus it is possible that CNTs could cause alterations in cell function without impacting viability.

Notably, we find that MWCNTs do not inhibit the capacity for HBMECs to form or maintain vessel-like structures. This result concurs with multiple studies that show carboxylated or amine functionalized CNTs (as opposed to pristine CNTs) do not greatly affect blood vessel integrity(Burke et al., 2011; Kafa et al., 2015; Ren et al., 2012; Wang et al., 2016). However, pristine SWCNTs cause dose dependent cytotoxicity and endothelial barrier dysfunction to human umbilical vein endothelial cell (HUVECs) monolayers(Rodríguez-Yáñez et al., 2015), and endothelial damage in vascular beds in mice(Burke et al., 2011). Furthermore, our findings are also consistent with other studies showing that MWCNT cytotoxicity is dependent upon the environment in which they are used, and more complex three-dimensional settings result in decreased cell sensitivity to CNT exposure compared to two-dimensional monolayer cultures (Behan et al., 2011; Eldridge et al., 2016; Movia et al., 2011).

We previously showed that acid oxidization of MWCNTs combined with coating with a 2% DSPE-PEG solution greatly increased the diffusion of MWCNTs through extracellular matrix (as compared to 1% DSPE-PEG, Pluronic F127 or uncoated MWCNTs) using brain

mimicking hydrogels, indicating that this type of nanotube was potentially useful for intracerebral applications including photothermal therapy of glioblastoma(Eldridge et al., 2016). Interestingly, we find that these 2% DSPE-PEG MWCNTs were more cytotoxic to HBMEC monolayers than uncoated MWCNTs. To evaluate if the increased toxicity of coated MWCNTs is due to differences in cellular uptake, we quantified percent uptake of uncoated and coated MWCNTs in HBMECs in monolayer and found that uncoated MWCNTs were taken up at a higher percent compared to coated MWCNTs. This increase in uptake of uncoated MWCNTs compared to coated MWCNTs may be due to the increased aggregation and sedimentation of the uncoated MWCNTs; however, it may be due to alternate cellular interactions caused by the coating. Our previous studies tracking the uptake of uncoated and DSPE-PEG-coated MWCNTs by breast cancer cells indicated that the uncoated tubes, which aggregate in culture media, were taken up by phagocytic pathways including macropinocytosis(Fahrenholtz et al., 2015). On the other hand, we found that direct piercing of the cell membrane played a role in uptake of DSPE-PEG coated tubes(Fahrenholtz et al., 2015). Others have shown that PEG-coated nanoparticles exhibit decreased uptake in a cervical cancer model (Sims et al., 2016) as well as various neural cell populations (microglia, astrocytes, neural stem cells) (Jenkins et al., 2016) relative to nanoparticles with other coatings. This indicates that a PEG-coating may actively decrease cell uptake due to changes in surface chemistry that may ultimately affect cellular interactions (Jenkins et al., 2016). Thus, the mechanism by which different types of MWCNTs translocate across cell membranes may influence their cytotoxicity. Ultimately, our present findings indicate that higher cellular uptake of MWCNTs does not necessarily correlate with increased toxicity. Because the high cytotoxicity of the DSPE-PEG coated MWCNTs we observed in HBMEC monolayers was not seen when HBMECs were grown on Matrigel, our data suggest that growth conditions can also significantly affect the toxicological responses of HBMECs to different types of MWCNTs.

Conclusions

In this paper, we present a modification of a commonly used viability assay (CellTiter-Glo®) that is effective to evaluate cell viability in a 2D and 3D setting without CNT interference. We show that MWCNTs do not influence HBMEC viability, induce apoptosis, decrease microvessel formation, or affect microvessel integrity when HBMECs are grown on Matrigel. In contrast, MWCNTs are cytotoxic to HBMECs grown directly on standard tissue culture plastic. These findings contribute to the field of nanotoxicology by validating methods of toxicological analysis in two dimensional and three dimensional cell models and promote an array of toxicity assays to evaluate cell viability with minimal interference by MWCNTs. Furthermore, based upon the available data, it appears that studies of MWCNT cytotoxicity in endothelial cell monolayers may not be predictive of *in vivo* outcomes, which supports further research into the use of tissue-mimicking endothelial cell culture models to help bridge this gap.

Supplementary Material

Refer to Web version on PubMed Central for supplementary material.

Acknowledgments

This work was supported by grant NCI R00CA154006 (R. S.) and by start-up funds from the Wake Forest School of Medicine Department of Cancer Biology. Assistance provided by the Wake Forest University Comprehensive Cancer Center Cell Viral Vector Core Laboratory was supported in part by NCI CCSG P30CA012197. We thank Jessica Swanner, Hugo Jimenez, and James Sears for assistance in data collection and analysis.

Funding to support this work was provided by grant NCI R00CA154006 (R. S.) and by start-up funds from the Wake Forest School of Medicine Department of Cancer Biology. Assistance provided by the Wake Forest University Comprehensive Cancer Center Cell Viral Vector Core Laboratory was supported in part by NCI CCSG P30CA012197. Dr. Singh has intellectual property related to the use of carbon nanotubes for treating cancerous tissue and, in particular, cancer stem cells, using carbon nanotubes and near infrared radiation (Patent# US20130304050 A1 “Methods for Treating Cancercerous Tissue”), and is developing additional intellectual property relating to other biomedical applications of carbon nanotubes.

References

Al-Jamal KT, Gherardini L, Bardi G, Nunes A, Guo C, Bussy C, Herrero MA, Bianco A, Prato M, Kostarelos K, Pizzorusso T. Functional motor recovery from brain ischemic insult by carbon nanotube-mediated siRNA silencing. Proc Natl Acad Sci U S A. 2011a; 108:10952–10957. [PubMed: 21690348]

Al-Jamal KT, Nerl H, Muller KH, Ali-Boucetta H, Li S, Haynes PD, Jinschek JR, Prato M, Bianco A, Kostarelos K, Porter AE. Cellular uptake mechanisms of functionalised multi-walled carbon nanotubes by 3D electron tomography imaging. Nanoscale. 2011b; 3:2627–2635. [PubMed: 21603701]

Alshehri R, Ilyas AM, Hasan A, Arnaout A, Ahmed F, Memic A. Carbon Nanotubes in Biomedical Applications: Factors, Mechanisms, and Remedies of Toxicity. J Med Chem. 2016

Arnaoutova I, Kleinman HK. In vitro angiogenesis: endothelial cell tube formation on gelled basement membrane extract. Nat Protoc. 2010; 5:628–635. [PubMed: 20224563]

Azad N, Iyer AK, Wang L, Liu Y, Lu Y, Rojanasakul Y. Reactive oxygen species-mediated p38 MAPK regulates carbon nanotube-induced fibrogenic and angiogenic responses. Nanotoxicology. 2013; 7:157–168. [PubMed: 22263913]

Bardi G, Nunes A, Gherardini L, Bates K, Al-Jamal KT, Gaillard C, Prato M, Bianco A, Pizzorusso T, Kostarelos K. Functionalized carbon nanotubes in the brain: cellular internalization and neuroinflammatory responses. PLoS One. 2013; 8:e80964. [PubMed: 24260521]

Behan BL, DeWitt DG, Bogdanowicz DR, Koppes AN, Bale SS, Thompson DM. Single-walled carbon nanotubes alter Schwann cell behavior differentially within 2D and 3D environments. Journal of biomedical materials research Part A. 2011; 96:46–57. [PubMed: 20949573]

Boulares AH, Yakovlev AG, Ivanova V, Stoica BA, Wang G, Iyer S, Smulson M. Role of poly(ADP-ribose) polymerase (PARP) cleavage in apoptosis. Caspase 3-resistant PARP mutant increases rates of apoptosis in transfected cells. J Biol Chem. 1999; 274:22932–22940. [PubMed: 10438458]

Brown RM, Meah CJ, Heath VL, Styles IB, Bicknell R. Tube-Forming Assays. Methods Mol Biol. 2016; 1430:149–157. [PubMed: 27172951]

Burke, AR., Singh, RN., Carroll, DL., Owen, JD., Kock, ND., D’Agostino, R., Jr, Torti, FM., Torti, SV. Biomaterials. Vol. 32. Elsevier Ltd; England: 2011. Determinants of the thrombogenic potential of multiwalled carbon nanotubes; p. 5970-5978.2011

Burke AR, Singh RN, Carroll DL, Wood JC, D’Agostino RB Jr, Ajayan PM, Torti FM, Torti SV. The resistance of breast cancer stem cells to conventional hyperthermia and their sensitivity to nanoparticle-mediated photothermal therapy. Biomaterials. 2012; 33:2961–2970. [PubMed: 22245557]

Bussy C, Al-Jamal KT, Boczkowski J, Lanone S, Prato M, Bianco A, Kostarelos K. Microglia Determine Brain Region-Specific Neurotoxic Responses to Chemically Functionalized Carbon Nanotubes. ACS nano. 2015; 9:7815–7830. [PubMed: 26043308]

Cellot G, Cilia E, Cipollone S, Rancic V, Sucapane A, Giordani S, Gambazzi L, Markram H, Grandolfo M, Scaini D, Gelain F, Casalis L, Prato M, Giugliano M, Ballerini L. Carbon nanotubes

might improve neuronal performance by favouring electrical shortcuts. Nat Nanotechnol. 2009; 4:126–133. [PubMed: 19197316]

Chen L, Xie H, Yu W. Functionalization Methods of Carbon Nanotubes and Its Applications. InTech. 2011

Chia SL, Tay CY, Setyawati MI, Leong DT. Biomimicry 3D gastrointestinal spheroid platform for the assessment of toxicity and inflammatory effects of zinc oxide nanoparticles. Small (Weinheim an der Bergstrasse, Germany). 2015; 11:702–712.

Cho WS, Thielbeer F, Duffin R, Johansson EM, Megson IL, MacNee W, Bradley M, Donaldson K. Surface functionalization affects the zeta potential, coronal stability and membranolytic activity of polymeric nanoparticles. Nanotoxicology. 2014; 8:202–211. [PubMed: 23379633]

Dal Bosco L, Weber GE, Parfitt GM, Cordeiro AP, Sahoo SK, Fantini C, Klosterhoff MC, Romano LA, Furtado CA, Santos AP, Monserrat JM, Barros DM. Biopersistence of PEGylated Carbon Nanotubes Promotes a Delayed Antioxidant Response after Infusion into the Rat Hippocampus. PloS one. 2015; 10:e0129156. [PubMed: 26075787]

Dubiak-Szepietowska M, Karczmarczyk A, Winckler T, Feller KH. A cell-based biosensor for nanomaterials cytotoxicity assessment in three dimensional cell culture. Toxicology. 2016; 370:60–69. [PubMed: 27693313]

Eldridge BN, Bernish BW, Fahrenholtz CD, Singh RN. Photothermal Therapy of Glioblastoma Multiforme Using Multiwalled Carbon Nanotubes Optimized for Diffusion in Extracellular Space. ACS Biomater Sci Eng. 2016; 2:963–976. [PubMed: 27795996]

Fahrenholtz CD, Hadimani M, King SB, Torti SV, Singh R. Targeting breast cancer with sugar-coated carbon nanotubes. Nanomedicine (Lond). 2015; 10:2481–2497. [PubMed: 26296098]

Herzog E, Casey A, Lyng FM, Chambers G, Byrne HJ, Davoren M. A new approach to the toxicity testing of carbon-based nanomaterials–the clonogenic assay. Toxicol Lett. 2007; 174:49–60. [PubMed: 17920791]

Jenkins SI, Weinberg D, al-Shakli AF, Fernandes AR, Yiu HHP, Telling ND, Roach P, Chari DM. 'Stealth' nanoparticles evade neural immune cells but also evade major brain cell populations: Implications for PEG-based neurotherapeutics. Journal of Controlled Release. 2016; 224:136–145. [PubMed: 26780172]

Jung S, Bang M, Kim BS, Lee S, Kotov NA, Kim B, Jeon D. Intracellular gold nanoparticles increase neuronal excitability and aggravate seizure activity in the mouse brain. PLoS One. 2014; 9:e91360. [PubMed: 24625829]

Kafa H, Wang JTW, Rubio N, Klippstein R, Costa PM, Hassan HAFM, Sosabowski JK, Bansal SS, Preston JE, Abbott NJ, Al-Jamal KT. Translocation of LRP1 targeted carbon nanotubes of different diameters across the blood–brain barrier in vitro and in vivo. Journal of Controlled Release. 2016; 225:217–229. [PubMed: 26809004]

Kafa H, Wang JTW, Rubio N, Venner K, Anderson G, Pach E, Ballesteros B, Preston JE, Abbott NJ, Al-Jamal KT. The interaction of carbon nanotubes with an in vitro blood-brain barrier model and mouse brain in vivo. Biomaterials. 2015; 53:437–452. [PubMed: 25890741]

Krug HF, Wick P. Nanotoxicology: an interdisciplinary challenge. Angewandte Chemie (International ed in English). 2011; 50:1260–1278. [PubMed: 21290492]

Lacerda L, Ali-Boucetta H, Kraszewski S, Tarek M, Prato M, Ramseyer C, Kostarelos K, Bianco A. How do functionalized carbon nanotubes land on, bind to and pierce through model and plasma membranes. Nanoscale. 2013; 5:10242–10250. [PubMed: 24056765]

Lacerda L, Russier J, Pastorin G, Herrero MA, Venturelli E, Dumortier H, Al-Jamal KT, Prato M, Kostarelos K, Bianco A. Translocation mechanisms of chemically functionalised carbon nanotubes across plasma membranes. Biomaterials. 2012; 33:3334–3343. [PubMed: 22289266]

Lee HJ, Park J, Yoon OJ, Kim HW, Lee DY, Kim do H, Lee WB, Lee NE, Bonventre JV, Kim SS. Amine-modified single-walled carbon nanotubes protect neurons from injury in a rat stroke model. Nat Nanotechnol. 2011; 6:121–125. [PubMed: 21278749]

Lee J, Lilly GD, Doty RC, Podsiadlo P, Kotov NA. In vitro toxicity testing of nanoparticles in 3D cell culture. Small. 2009; 5:1213–1221. [PubMed: 19263430]

Lee, W., Parpura, V. Chapter 6 - Carbon nanotubes as substrates/scaffolds for neural cell growth. In: Hari Shanker, S., editor. Progress in Brain Research. Vol. 180. Elsevier; 2009. p. 110-125.

Leite PE, Pereira MR, Granjeiro JM. Hazard effects of nanoparticles in central nervous system: Searching for biocompatible nanomaterials for drug delivery. Toxicol In Vitro. 2015; 29:1653–1660. [PubMed: 26116398]

Madani SY, Naderi N, Dissanayake O, Tan A, Seifalian AM. A new era of cancer treatment: carbon nanotubes as drug delivery tools. Int J Nanomedicine. 2011; 6:2963–2979. [PubMed: 22162655]

Mattson MP, Haddon RC, Rao AM. Molecular functionalization of carbon nanotubes and use as substrates for neuronal growth. Journal of Molecular Neuroscience. 2000; 14:175–182. [PubMed: 10984193]

Meng J, Li X, Wang C, Guo H, Liu J, Xu H. Carbon nanotubes activate macrophages into a M1/M2 mixed status: recruiting naive macrophages and supporting angiogenesis. ACS applied materials & interfaces. 2015; 7:3180–3188. [PubMed: 25591447]

Meng L, Jiang A, Chen R, Li CZ, Wang L, Qu Y, Wang P, Zhao Y, Chen C. Inhibitory effects of multiwall carbon nanotubes with high iron impurity on viability and neuronal differentiation in cultured PC12 cells. Toxicology. 2013; 313:49–58. [PubMed: 23219591]

Min JO, Kim SY, Shin US, Yoon BE. Multi-walled carbon nanotubes change morpho-functional and GABA characteristics of mouse cortical astrocytes. Journal of nanobiotechnology. 2015; 13:92. [PubMed: 26683698]

Monteiro-Riviere NA, Inman AO, Zhang LW. Limitations and relative utility of screening assays to assess engineered nanoparticle toxicity in a human cell line. Toxicology and applied pharmacology. 2009; 234:222–235. [PubMed: 18983864]

Movia D, Prina-Mello A, Bazou D, Volkov Y, Giordani S. Screening the cytotoxicity of single-walled carbon nanotubes using novel 3D tissue-mimetic models. ACS nano. 2011; 5:9278–9290. [PubMed: 22017733]

Muoth C, Wichser A, Monopoli M, Correia M, Ehrlich N, Loeschner K, Gallud A, Kucki M, Diener L, Manser P, Jochum W, Wick P, Buerki-Thurnherr T. A 3D co-culture microtissue model of the human placenta for nanotoxicity assessment. Nanoscale. 2016; 8:17322–17332. [PubMed: 27714104]

Nafee N, Schneider M, Schaefer UF, Lehr CM. Relevance of the colloidal stability of chitosan/PLGA nanoparticles on their cytotoxicity profile. International journal of pharmaceutics. 2009; 381:130–139. [PubMed: 19450671]

O'Brien LE, Zegers MM, Mostov KE. Opinion: Building epithelial architecture: insights from three-dimensional culture models. Nature reviews Molecular cell biology. 2002; 3:531–537. [PubMed: 12094219]

Ouyang M, White EE, Ren H, Guo Q, Zhang I, Gao H, Yanyan S, Chen X, Weng Y, Da Fonseca A, Shah S, Manuel ER, Zhang L, Vonderfecht SL, Alizadeh D, Berlin JM, Badie B. Metronomic Doses of Temozolomide Enhance the Efficacy of Carbon Nanotube CpG Immunotherapy in an Invasive Glioma Model. PLoS One. 2016; 11:e0148139. [PubMed: 26829221]

Palencia S, Vera S, Diez-Pascual AM, San Andres MP. Quenching of fluorene fluorescence by single-walled carbon nanotube dispersions with surfactants: application for fluorene quantification in wastewater. Analytical and bioanalytical chemistry. 2015; 407:4671–4682. [PubMed: 25893803]

Pampaloni F, Reynaud EG, Stelzer EH. The third dimension bridges the gap between cell culture and live tissue. Nature reviews Molecular cell biology. 2007; 8:839–845. [PubMed: 17684528]

Pantarotto D, Singh R, McCarthy D, Erhardt M, Briand JP, Prato M, Kostarelos K, Bianco A. Functionalized carbon nanotubes for plasmid DNA gene delivery. Angew Chem Int Ed Engl. 2004; 43:5242–5246. [PubMed: 15455428]

Ren J, Shen S, Wang D, Xi Z, Guo L, Pang Z, Qian Y, Sun X, Jiang X. The targeted delivery of anticancer drugs to brain glioma by PEGylated oxidized multi-walled carbon nanotubes modified with angiopep-2. Biomaterials. 2012; 33:3324–3333. [PubMed: 22281423]

Rodríguez-Yáñez Y, Bahena-Uribe D, Chávez-Munguía B, López-Marure R, González-Monroy S, Cisneros B, Albores A. Commercial single-walled carbon nanotubes effects in fibrinolysis of human umbilical vein endothelial cells. Toxicology in Vitro. 2015; 29:1201–1214. [PubMed: 25790727]

Santos T, Fang X, Chen MT, Wang W, Ferreira R, Jhaveri N, Gundersen M, Zhou C, Pagnini P, Hofman FM, Chen TC. Sequential administration of carbon nanotubes and near-infrared radiation for the treatment of gliomas. Front Oncol. 2014; 4:180. [PubMed: 25077069]

Sims LB, Curtis LT, Frieboes HB, Steinbach-Rankins JM. Enhanced uptake and transport of PLGA-modified nanoparticles in cervical cancer. J Nanobiotechnology. 2016; 14:33. [PubMed: 27102372]

Singh R, Pantarotto D, McCarthy D, Chaloin O, Hoebeke J, Partidos CD, Briand JP, Prato M, Bianco A, Kostarelos K. Binding and condensation of plasmid DNA onto functionalized carbon nanotubes: toward the construction of nanotube-based gene delivery vectors. J Am Chem Soc. 2005; 127:4388–4396. [PubMed: 15783221]

Singh R, Torti SV. Carbon nanotubes in hyperthermia therapy. Adv Drug Deliv Rev. 2013; 65:2045–2060. [PubMed: 23933617]

Stocke NA, Sethi P, Jyoti A, Chan R, Arnold SM, Hilt JZ, Upreti M. Toxicity evaluation of magnetic hyperthermia induced by remote actuation of magnetic nanoparticles in 3D micrometastasic tumor tissue analogs for triple negative breast cancer. Biomaterials. 2017; 120:115–125. [PubMed: 28056401]

Truong L, Moody IS, Stankus DP, Nason JA, Lonergan MC, Tanguay RL. Differential stability of lead sulfide nanoparticles influences biological responses in embryonic zebrafish. Archives of toxicology. 2011; 85:787–798. [PubMed: 21140132]

Wang, CH., Chiou, SH., Chou, CP., Chen, YC., Huang, YJ., Peng, CA. Nanomedicine. Vol. 7. Elsevier Inc; United States: 2011. Photothermolysis of glioblastoma stem-like cells targeted by carbon nanotubes conjugated with CD133 monoclonal antibody; p. 69-79.2011

Wang JT, Rubio N, Kafa H, Venturelli E, Fabbro C, Menard-Moyon C, Da Ros T, Sosabowski JK, Lawson AD, Robinson MK, Prato M, Bianco A, Festy F, Preston JE, Kostarelos K, Al-Jamal KT. Kinetics of functionalised carbon nanotube distribution in mouse brain after systemic injection: Spatial to ultra-structural analyses. Journal of controlled release: official journal of the Controlled Release Society. 2016; 224:22–32. [PubMed: 26742944]

Wierzbicki M, Sawosz E, Grodzik M, Prasek M, Jaworski S, Chwalibog A. Comparison of anti-angiogenic properties of pristine carbon nanoparticles. Nanoscale research letters. 2013; 8:195. [PubMed: 23618362]

Wills JW, Hondow N, Thomas AD, Chapman KE, Fish D, Maffeis TG, Penny MW, Brown RA, Jenkins GJ, Brown AP, White PA, Doak SH. Genetic toxicity assessment of engineered nanoparticles using a 3D in vitro skin model (EpiDerm). Part Fibre Toxicol. 2016; 13:50. [PubMed: 27613375]

Worle-Knirsch JM, Pulskamp K, Krug HF. Oops they did it again! Carbon nanotubes hoax scientists in viability assays. Nano Lett. 2006; 6:1261–1268. [PubMed: 16771591]

Yamada KM, Cukierman E. Modeling tissue morphogenesis and cancer in 3D. Cell. 2007; 130:601–610. [PubMed: 17719539]

Zhang Y, Xu Y, Li Z, Chen T, Lantz SM, Howard PC, Paule MG, Slikker W Jr, Watanabe F, Mustafa T, Biris AS, Ali SF. Mechanistic toxicity evaluation of uncoated and PEGylated single-walled carbon nanotubes in neuronal PC12 cells. ACS nano. 2011; 5:7020–7033. [PubMed: 21866971]

Zhao D, Alizadeh D, Zhang L, Liu W, Farrukh O, Manuel E, Diamond DJ, Badie B. Carbon nanotubes enhance CpG uptake and potentiate antiglioma immunity. Clin Cancer Res. 2011; 17:771–782. [PubMed: 21088258]

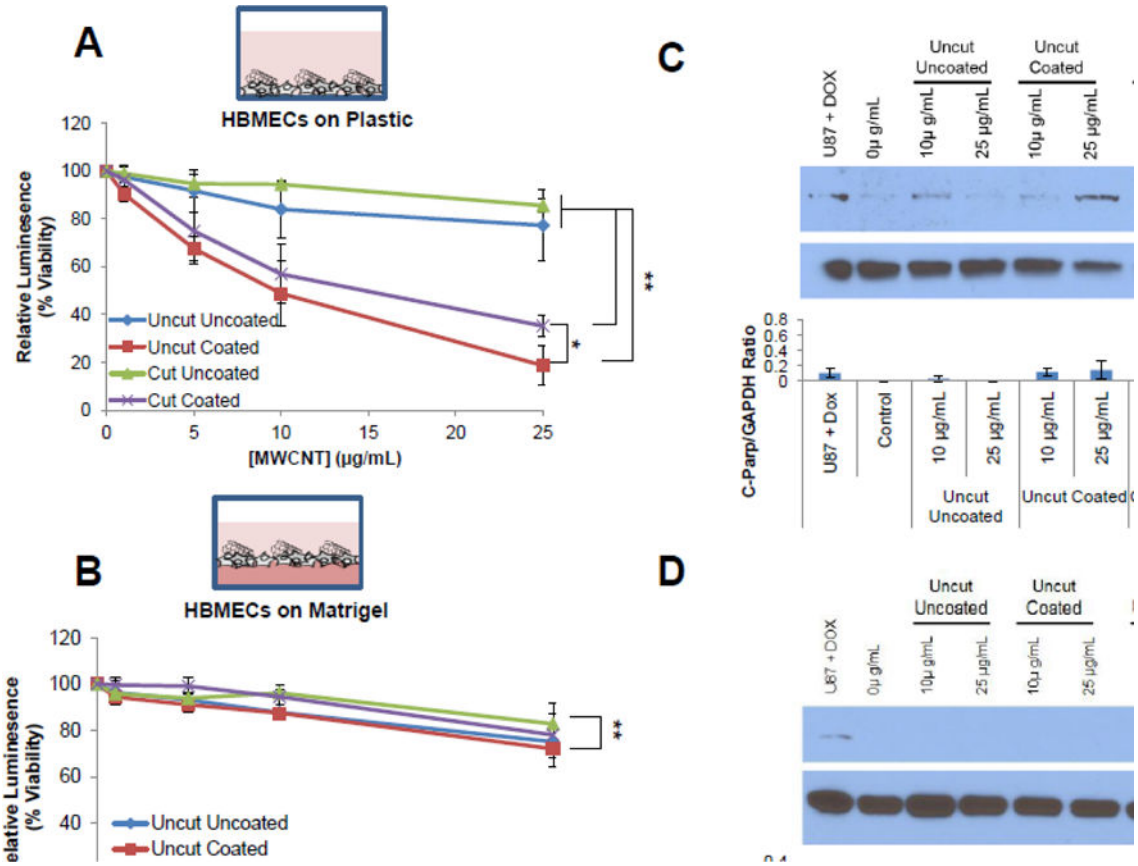

Figure 1. Evaluation of the cytotoxicity induced by MWCNTs on HBMECs grown on plastic or matrigel

HBMECs were plated on standard tissue culture plastic or matrigel coated plastic and recovered overnight. HBMECs grown on plastic (A) or Matrigel (B) were treated for 24 h with increasing doses of different types of MWCNTs as indicated. Cells were lysed, pelleted, and the supernatant was analyzed for ATP content as a measure of cell viability using the CellTiter-Glo assay. Three independent biological replicates were performed with at least three technical replicates per treatment group. Endpoint analysis shows the groups that are significantly different (*p≤0.05, **p≤0.01) at the highest dose (ANOVA; post-hoc T-Test). In parallel, lysates of similarly treated cells grown on plastic (C) or Matrigel (D) were collected and probed for cleaved PARP, a protein indicative of apoptosis, via western blot analysis. GAPDH was used as a loading control. Lysates from U87 cells treated with 10 μM doxorubicin was used as a positive control. Cells grown on matrigel were isolated using dispase to degrade the matrigel without affecting HBMEC cell integrity. The graph below the western blot displays average fold change of cleaved PARP protein levels relative to GAPDH loading control for three independent biological replicates. Fold change is displayed as the mean ± standard deviation of each experiment.

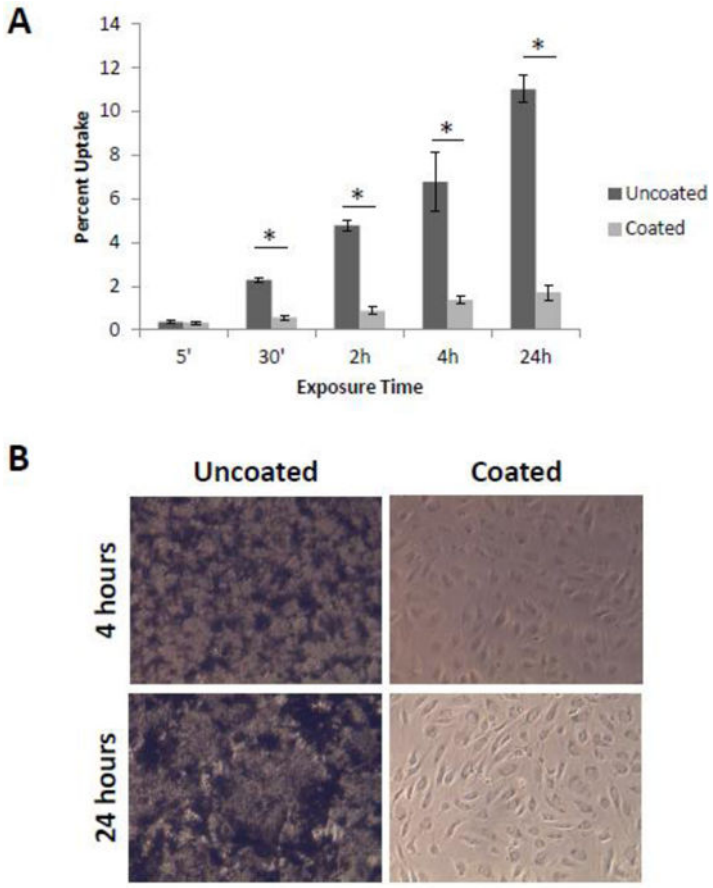

Figure 2. Evaluation of uncoated or coated MWCNT uptake in HBMECs

HBMECs were plated on plastic to form monolayers and treated the following day with cut uncoated ^{3}H-MWCNT, cut DSPE-PEG coated ^{3}H-MWCNT, or vehicle for the specified times. (A) Cells were washed twice in ice cold PBS, harvested in lysis buffer, and ^{3}H activity was assessed using a scintillation counter. Percent uptake was calculated based on input decays per minute. Three samples were used for each condition and the data are displayed as the mean ± standard error of each measurement. (B) Images taken after 24 h treatment show increased aggregation and sedimentation of uncoated MWCNTs on to HBMECs. By comparison, no aggregated or sedimented cut, DSPE-PEG coated MWCNTs are apparent. *$p<0.05$ (T-Test).

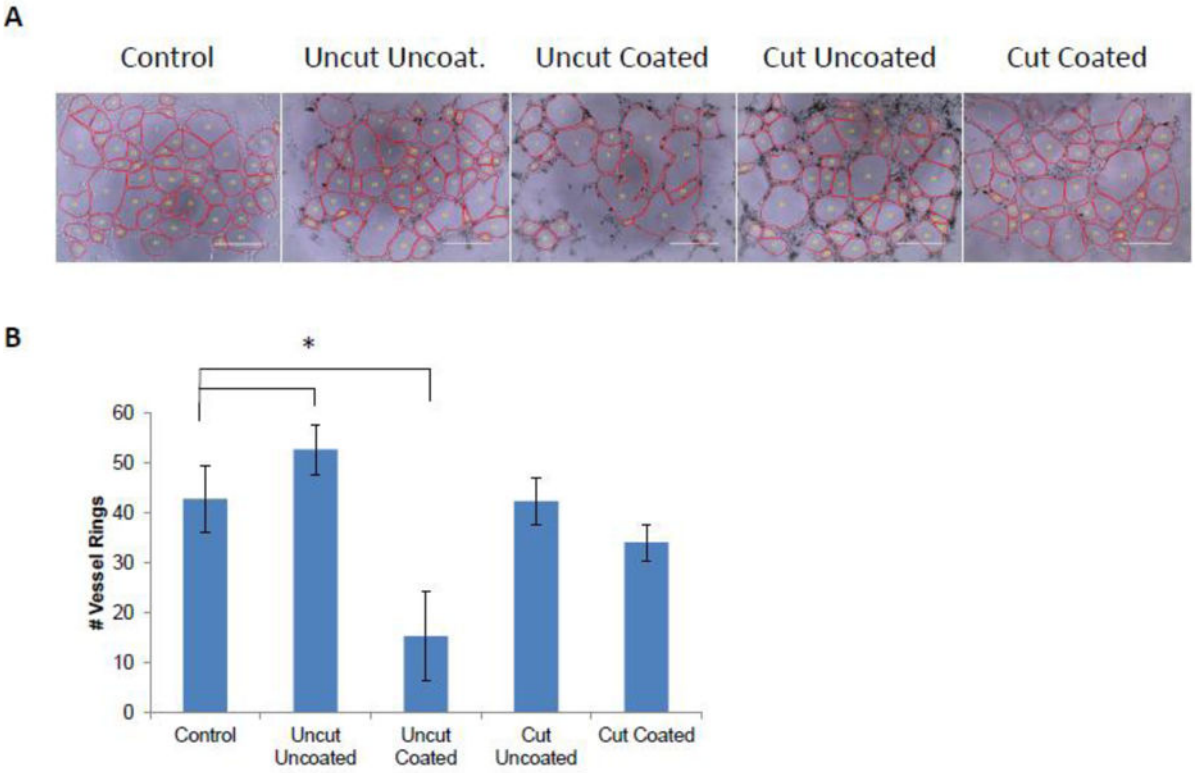

Figure 3. Tube Formation Assay of MWCNT-treated HBMECs

HBMECs were treated in monolayer overnight with 25 μg/mL of each type of MWCNTs and then were replated on matrigel to induce tube formation. After 6 h, photomicrographs of tube formation were taken. Representative images are shown in (A). The average number of HBMEC vessel rings was quantified in three independent biological replicates, with each biological replicate containing triplicate technical replicates. Data are displayed as the mean ± standard error of each experiment (B). Significant differences among groups are indicated: *$p<0.05$ (ANOVA; post-hoc T-Test).

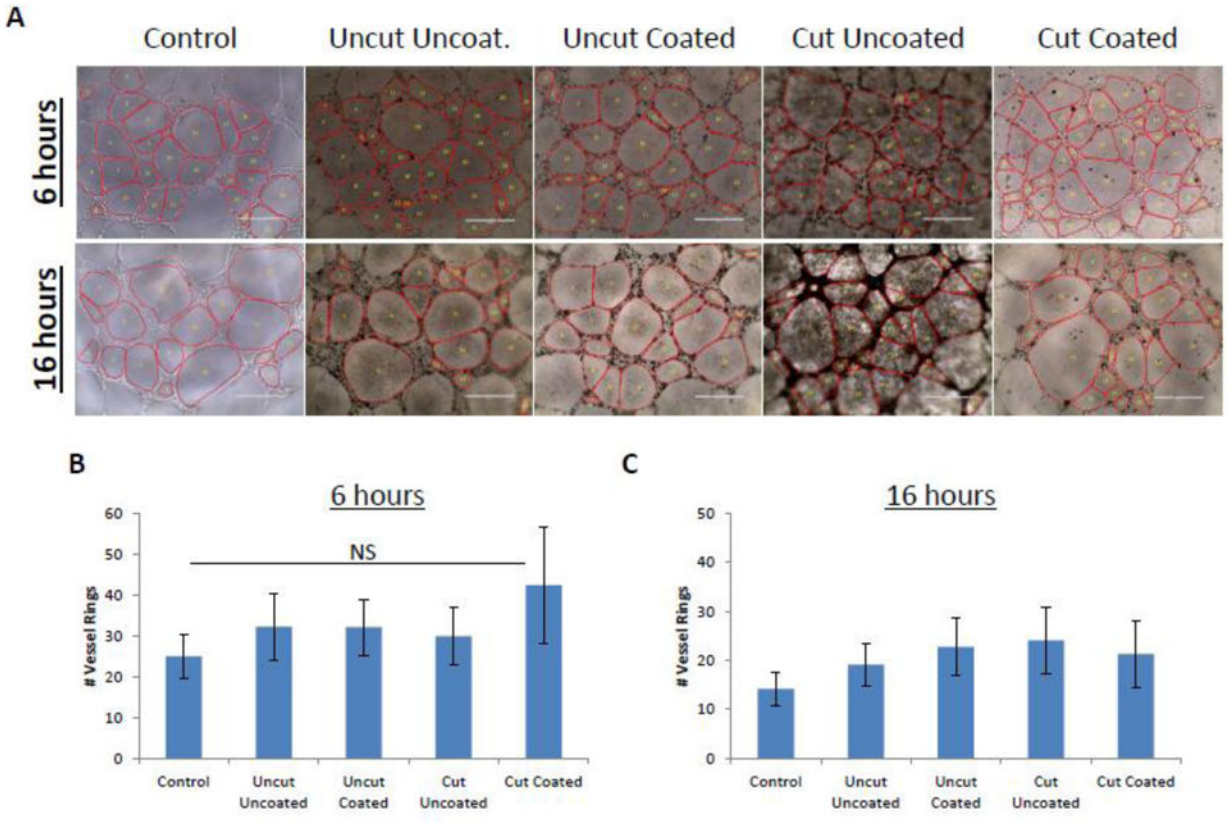

Figure 4. Treatment of HBMEC tubes with MWCNTs

HBMECs were plated in triplicate on matrigel and allowed to form tube structures, followed by treatment with 25 μg/mL of each type of MWCNT. After 6 h and 16 h, photomicrographs of tube formation were taken. Representative images are shown in (A) for a single biological replicate. The average number of HBMEC vessel rings was quantified and measured in three independent biological replicates, with each biological replicate containing triplicate technical replicates. Data are displayed as the mean ± standard deviation of each experiment (B and C). No significant ($p>0.05$) difference among groups was detected (ANOVA).

Table 1

Physicochemical characterization of MWCNTs

		Uncut		Cut (Acid Oxidized)	
	Dispersant	**Uncoated**	**Coated (2% DSPE-PEG)**	**Uncoated**	**Coated (2% DSPE-PEG)**
Hydrodynamic diameter (D)/ Polydispersity index (PI)	**H_2O**	D=185 ± 2 nm	D=251 ± 13 nm	D=137 ± 0.1 nm	D=171 ± 0.4 nm
		PI=0.29 ± 0.02	PI=0.34 ± 0.02	PI=0.27 ± 0.01	PI=0.25 ± 0.01
	PBS	D=2086 ± 333 nm	D=219 ± 12 nm	D=709 ± 126 nm	D=166 ± 0.6 nm
		PI=0.55 ± 0.04	PI=0.38 ± 0.08	PI=0.31± 0.02	PI=0.22 ± 0.02
ζ-potential	**H_2O**	−37.9 ± 0.5 mV	−32.9 ± 0.9 mV	−49.3 ± 1.0 mV	−37.2 ± 0.6 mV